

Solubility of CO₂ in 15, 30, 45 and 60 mass% MEA from 40 to 120 °C and model representation using the extended UNIQUAC framework

Ugochukwu E. Aronu^a, Shahla Gondal^a, Erik T. Hessen^a, Tore Haug-Warberg^a, Ardi Hartono^a, Karl A. Hoff^b, Hallvard F. Svendsen^{a,*}

^a Department of Chemical Engineering, Norwegian University of Science and Technology, N-7491 Trondheim, Norway

^b SINTEF Materials and Chemistry, N-7465 Trondheim, Norway

ARTICLE INFO

Article history:

Received 23 January 2011

Received in revised form

20 August 2011

Accepted 27 August 2011

Available online 3 September 2011

Keywords:

CO₂ absorption

Separations

Phase equilibria

Thermodynamic process

Extended UNIQUAC

Monoethanolamine (MEA)

ABSTRACT

New experimental data for vapor–liquid equilibrium of CO₂ in aqueous monoethanolamine solutions are presented for 15, 30, 45 and 60 mass% MEA and from 40 to 120 °C. CO₂ partial pressures over loaded MEA solutions were measured using a low temperature equilibrium apparatus while total pressures were measured with a high temperature equilibrium apparatus. Experimental data are given as CO₂ partial pressure as function of loading in solution for temperatures from 40 to 80 °C and as total pressures for temperatures from 60 to 120 °C for the different MEA concentrations. The extended UNIQUAC model framework was applied and model parameters were fitted to the new experimental VLE data and physical CO₂ solubility data from the literature. The model gives a good representation of the experimental VLE data for CO₂ partial pressures and total pressures for all MEA concentrations with an average absolute relative deviation (AARD) of 24.3% and 11.7%, respectively, while the physical solubility data were represented with an AARD of 2.7%. Further, the model predicts well literature data on freezing point depression, excess enthalpy and liquid phase speciation determined by NMR.

© 2011 Elsevier Ltd. All rights reserved.

1. Introduction

Scrubbing effluent industrial fluid streams of acid gases such as CO₂ and H₂S is an important industrial process operation. The technique has historically been applied for various reasons such as improving the calorific value of gas streams and avoiding corrosion on process lines and fittings. Recently, a more compelling reason for scrubbing of carbon dioxide from process streams has been the urgent need to reduce greenhouse gas emissions. CO₂ capture by absorption technology remains the most promising and most mature technology for CO₂ removal from exhaust gas streams, and reducing the cost of this technology is of global interest. Amine-based CO₂ solvents have been the most studied absorbents for CO₂ capture by absorption.

Several studies have been carried out on the solubility of CO₂ in aqueous MEA solution. Tables presenting summaries of previous studies were presented by Jou et al. (1995), Kohl and Nielsen (1997) and Ma'mun et al. (2005). The experimental data of Jou et al. (1995) covers a wide range of temperatures, pressures and loadings, however it is available only for 30 mass% MEA. Of all the numerous work on MEA, only Mason and Dodge (1936) and Atadan (1954) measured CO₂ solubility in MEA at concentrations

higher than 30 mass%. These data are old and quite few. Mason and Dodge (1936) measured only up to 75 °C and between 1.3 and 100 kPa while Atadan (1954) measured up to 70 °C and between 103 and 3447 kPa, thus not covering the temperature range for regeneration. There is also a strong need for more data in the very low loading and pressure regions for modeling purposes. Further MEA is often used as a base case solvent in comparative studies of new solvents for CO₂ absorption and new processes applying higher solvent concentrations are being developed. For e.g. Bouillon et al. (2011) have shown that use of MEA at higher concentrations can give improved CO₂ absorption results. Thus an up-to-date robust VLE data set for H₂O–MEA–CO₂ system, spanning a large concentration range, is clearly needed.

Accurate correlation of equilibrium behavior of CO₂ in aqueous MEA solutions will enable better process simulations towards cost reduction, better column design as well as improved plant operation. Different thermodynamic models have been used to describe the equilibrium behavior of CO₂ in aqueous alkanolamine solutions, in particular, MEA. These models could be categorized into three (Hessen et al., 2010); the non-rigorous models, e.g. Kent-Eisenberg (1976) and the rigorous models with the two branches; activity models (excess Gibbs energy) and equation of state models (Helmholtz energy). Activity based models vary in complexity, ranging from the relatively simple Deshmukh and Mather (1981) to the more sophisticated ones, such as electrolyte–NRTL (Chen et al., 1982; Chen and Evans, 1986) and extended UNIQUAC models (Nicolaisen et al., 1993; Thomsen, 1997; Thomsen and Rasmussen,

* Corresponding author. Tel.: +47 73594100; fax: +47 73594080.

E-mail addresses: ugochukwu.aronu@chemeng.ntnu.no (U.E. Aronu), hallvard.svendsen@chemeng.ntnu.no (H.F. Svendsen).

1999) models. The extended-UNIQUAC model was used in this work. Previous work such as Austgen et al. (1989), Faramarzi et al. (2009), Hessen et al. (2010), etc. have, respectively, implemented the original electrolyte–NRTL, refined electrolyte–NRTL and extended-UNIQUAC models for the H₂O–MEA–CO₂ system. However, all the implementations were based on experimental data of not more than 30 mass% MEA concentration, except for Hessen et al. (2010) who applied the r-e-NRTL to predict experimental VLE results of 60 mass% MEA up to 80 °C. None of the existing models have used the solubility of N₂O in MEA which by utilizing the so-called N₂O analogy (originally proposed by Clarke (1964) and verified by Laddha et al. (1981)) gives a measure of the physical solubility, or Henry's law constant, of CO₂ in the aqueous MEA solution. Through the physical solubility of CO₂, the activity coefficient of CO₂ can be calculated. In Hessen (2010) it was shown that existing models give CO₂ activity coefficients which are far from the N₂O analogy derived values.

The objectives of this work are to present a consistent VLE data set for MEA through experimental VLE measurements for 15, 30, 45 and 60 mass% MEA in the low and high CO₂ loading regions from 40 to 120 °C, and to use these data together with CO₂ solubility data based on the N₂O analogy, to provide a rigorous equilibrium model based on the extended UNIQUAC model framework.

2. Equilibrium experiments

2-Aminoethanol (MEA) (purity ≥ 99 mass%) was obtained from Sigma-Aldrich. Sample solutions of 15, 30, 45 and 60 mass% MEA were prepared using deionized water. A total of about 5.0 L solution of each MEA concentration was prepared. Solutions were prepared using a Sartorius GMBH Göttingen balance within ± 0.1 g. The gases used; CO₂, purity > 99.99 mol% and calibration gases, 2.5 mol% CO₂ and 4.96 mol% CO₂ were supplied by AGA Gas GmbH while N₂, purity > 99.999 mol% and calibration gas 100 ppm CO₂ were supplied by Yara Praxair AS.

2.1. Low temperature/atmospheric VLE apparatus

Vapor–liquid equilibrium for the CO₂ loaded MEA systems from 40 to 80 °C and at atmospheric pressure were measured using a low temperature/atmospheric vapor–liquid equilibrium apparatus (see Fig. 1), designed to operate up to 80 ± 0.1 °C. A volume of 150 cm³ of pre-loaded sample solutions were placed in three equilibrium cells, respectively (360 cm³ glass flasks) and flushed with N₂ gas to remove any dissolved oxygen. The gas phase was thereafter circulated by a BÜHLER pump (model P2) at a set temperature and analyzed online until steady values of gas phase

CO₂ composition were recorded by a calibrated Fisher–Rosemount BINOS[®] 100 NDIR Gas Analyzer. The gas phase was circulated typically for 20 min. Six different analyzers were used; 0–200 ± 2 ppm, 0–1000 ± 10 ppm, 0–2000 ± 20 ppm, 0–1 ± 0.01%, 0–5 ± 0.01%; 0–20 ± 0.1%. Analyzers were calibrated every day before measurements using certified calibration gases and gas mixtures of CO₂ and N₂ produced using a Bronkhorst Hi-Tec EL-Flow mass flow meter controller. The number of calibration points used in each analyzer range are given in Table 1. Three K-type thermocouples recorded the temperatures in the cell, the water bath and the gas phase temperature between the condenser and the analyzer, respectively, within ± 0.1 °C. Liquid phase compositions were obtained by taking a ~25 cm³ sample from cell 4 for CO₂ analysis by the barium chloride method and for total alkalinity. The liquid phases in all the cells are then removed and diluted with fresh solution or loaded with more CO₂ to change to a new loading, then shaken vigorously and refilled into the equilibrium cells for a new measurement. The amount of CO₂ pre-loaded was estimated using PG5002-S Delta Range balance from Mettler Toledo within ± 0.01 g. However, all solutions were analyzed using the BaCl₂ method where all gravimetric operations were carried out using a Mettler PM1200 from Mettler Toledo within ± 0.001 g. The apparatus has been described in detail by Ma'mun et al. (2005, 2006) and was used by Aronu et al. (2011a,b) for VLE measurements of amino acid based absorbents.

The apparatus circulates the gas through the liquid phase holding cells until equilibrium is reached. A gas phase bleed is extracted for composition measurement and then returned to the circulation loop. The extracted bleed is cooled to 10–15 °C to condense water and amine and the CO₂ content determined directly by the NDIR analyzers. The vapor phase will therefore consist of CO₂, N₂, and small amounts of H₂O and amine. The CO₂ molfraction in the analyzer is given by

$$y_{\text{CO}_2}^{\text{IR}} = \frac{n_{\text{CO}_2}^{\text{IR}}}{n_{\text{CO}_2}^{\text{IR}} + n_{\text{N}_2}^{\text{IR}} + n_{\text{H}_2\text{O}}^{\text{IR}} + n_{\text{amine}}^{\text{IR}}} \quad (1)$$

Table 1

Number of calibration points used for each CO₂ IR analyzer range.

CO ₂ analyzer concentration range	No. of calibration points in range
0–200 ppm	2
0–1000 ppm	2
0–2000	5
0–1.0%	5
0–5.0%	6
0–20.0%	8

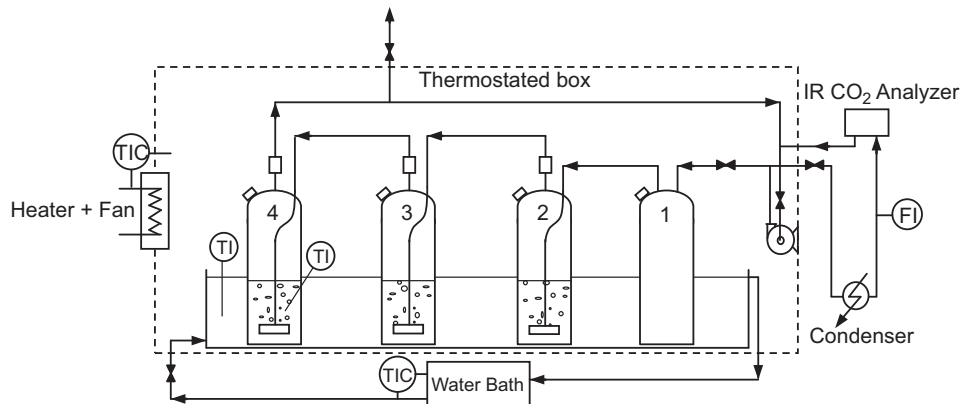


Fig. 1. Low temperature/atmospheric vapor–liquid equilibrium apparatus, Ma'mun et al. (2006).

where n is the molar flow and the superscript IR is the vapor phase in the IR analyzer. As non-condensable gases, the flows of CO₂ and N₂ before and after the condenser are assumed to be the same. The amount and CO₂ content in the condensate was checked and was found to have a negligible influence on the results even at low CO₂ partial pressures. Eq. (1) together with a mole balance gives the molar flow of CO₂ in the system as

$$y_{\text{CO}_2}^{\text{IR}} = \frac{n_{\text{CO}_2}}{n_{\text{tot}} - (n_{\text{H}_2\text{O}} - n_{\text{H}_2\text{O}}^{\text{IR}}) - (n_{\text{MEA}} - n_{\text{MEA}}^{\text{IR}})} \quad (2)$$

where n_{tot} , $n_{\text{H}_2\text{O}}$, and n_{MEA} , respectively, denote the total molar flow and the molar flows of H₂O and MEA in the circulation system. By dividing by the total pressure P , Eq.(2), the IR analyzer CO₂ mole fraction can be expressed as

$$y_{\text{CO}_2}^{\text{IR}} = p_{\text{CO}_2} / [P - (p_{\text{H}_2\text{O}} - p_{\text{H}_2\text{O}}^{\text{IR}}) - (p_{\text{MEA}} - p_{\text{MEA}}^{\text{IR}})] \quad (3)$$

Due to the low vapor pressure of most amines at cooler temperature, $p_{\text{MEA}}^{\text{IR}}$ is usually negligible. The partial pressures $p_{\text{H}_2\text{O}}$, $p_{\text{H}_2\text{O}}^{\text{IR}}$, p_{MEA} , $p_{\text{MEA}}^{\text{IR}}$ are determined from the model but can with negligible loss in precision also be determined using Raoult's law.

2.2. High temperature equilibrium measurement

Equilibrium total pressure data in the temperature range 60–120 °C for the systems were obtained using a high temperature VLE apparatus (Fig. 2). The apparatus consists of two connected autoclaves (1000 and 200 cm³) rotating 180° with 2 rpm and designed to operate up to 10.5 bar and 150 °C. Temperature and pressure were measured with two K-type thermocouples and a Druck PTX 610 pressure transducer, respectively. Equilibrium was obtained when the temperature and pressure were constant to within ±0.2 °C and ±0.1 kPa, respectively. This took about 4–6 h. The experiment starts when the cell is evacuated and purged with CO₂. Unloaded solution is then injected into the reactor through a liquid line and pure CO₂ is loaded at the desired temperature and at a set pressure. The CO₂ feed line is closed after about 1 h of loading. When equilibrium is

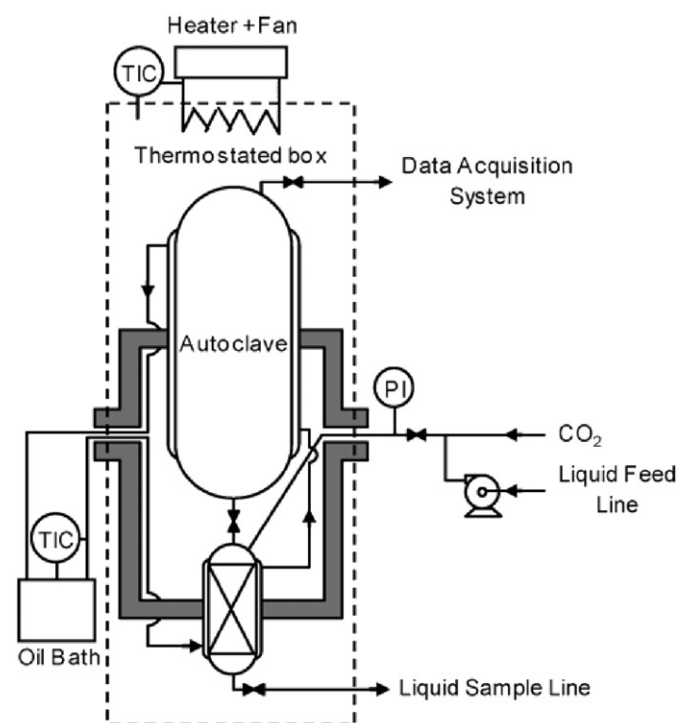


Fig. 2. High temperature equilibrium apparatus, Ma'mun et al. (2005).

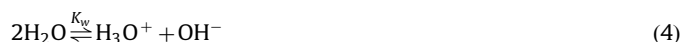
reached, i.e. when temperature and pressure are constant, a liquid sample for analysis is collected by closed sampling into a sampling cylinder containing about 100 mL of fresh solution. This immediately reduces the CO₂ pressure and CO₂ loss is avoided. The cylinder is weighed before and after sampling and cooled below ambient temperature in a refrigerator. This ensures no loss of CO₂ by flashing at atmospheric pressure. The actual CO₂ loading is determined by titration analysis and a mass balance. The data acquisition system uses Field Point Labview. Further details on the apparatus are given in Ma'mun et al. (2005).

3. Chemical and phase equilibrium

3.1. Chemical equilibrium

For a ternary H₂O–CO₂–amine system where the amine has a single amine functionality, like MEA, the following equilibrium reactions are expected:

Dissociation of water:



Dissociation of carbon dioxide:



Dissociation of bicarbonate:



Dissociation of protonated amine, MEA:



Carbamate reversion to bicarbonate:



Equilibrium reactions (4)–(8) are relevant for modeling of the equilibrium for the H₂O–MEA–CO₂ system. The equilibrium point of the reaction system was found using a non-stoichiometric Gibbs energy minimization routine (Hessen, 2010).

3.2. Vapor–liquid equilibrium

For a complete model of the MEA system, chemical equilibrium and vapor–liquid equilibrium must be solved simultaneously. The system is formulated as a standard VLE problem through the thermodynamic equilibrium criterion at given temperature and pressure.

$$\mu_i^{\text{vap}}(T, P, n) = \mu_i^{\text{liq}}(T, P, n) \quad (9)$$

where μ_i^{vap} and μ_i^{liq} are the chemical potentials of the species i in the vapor and liquid phase, respectively. The activity coefficients for species in the liquid phase were determined using the extended UNIQUAC framework and used in the phase equilibrium calculations. The Soave–Redlich–Kwong equation of state was used to calculate the gas phase properties. The equilibrium distribution of the volatile solute, CO₂, between the vapor and liquid was modeled based on Henry's law constant in water at system pressure and temperature as reference state. Because of the asymmetric reference state of CO₂, its phase equilibrium was calculated from

$$\phi_{\text{CO}_2} y_{\text{CO}_2} P = \gamma_{\text{CO}_2} x_{\text{CO}_2} H_{\text{CO}_2}^\infty \exp\left(\frac{v_{\text{CO}_2}^\infty (P - P_{\text{H}_2\text{O}}^S)}{RT}\right) \quad (10)$$

where γ_{CO_2} and ϕ_{CO_2} are the activity and the fugacity coefficients of CO₂, respectively, P the total pressure, $H_{\text{CO}_2}^\infty$ is the Henry's law

constant in water (Chen et al., 1979), $v_{\text{CO}_2}^\infty$ the infinite dilution partial molar volume of CO₂ (Brelvi and O'Connell, 1972) and T (K) is temperature. The reference states for water and amine were the pure components at system temperature and pressure. Thus the phase equilibrium was calculated from

$$\phi_i y_i P = \gamma_i x_i P_i \phi_i^s \exp\left(\frac{v_i(P - P_i^s)}{RT}\right) \quad (11)$$

Here γ_i , ϕ_i , ϕ_i^s are the activity coefficient, fugacity coefficients and saturated vapor fugacity coefficients, respectively, while v_i is the partial molar volumes for the components (DIPPR, 2004).

The standard chemical potentials for most of the species in the CO₂-amine system are not readily available in the literature. However, the equilibrium constant for the reaction j is related to the standard chemical potentials, μ_i^0 , through Eq. (12) which allows for a calculation of the standard state chemical potentials.

$$RT \ln K_j(T) = -\sum_i \nu_{ij} \mu_i^0(T) \quad (12)$$

For the H₂O–MEA–CO₂ system there are nine species and four reactions, hence Eq. (12) is underspecified. This was resolved by setting four of the standard state chemical potentials to zero and then solving for the remaining ones. This solution approach has been described by Smith and Missen (1982), Solbraa (2002), and Hessen et al. (2010).

3.3. Activity coefficient model

The activity coefficients for all species were calculated using the extended UNIQUAC thermodynamic model framework. The original non-electrolyte UNIQUAC equation by Abrams and Prausnitz (1975) was extended for electrolyte systems by addition of an electrostatic term by Sanders et al. (1986) to a modified UNIQUAC equation. The model framework implemented in this work is as presented by Thomsen (1997) and Thomsen and Rasmussen (1999). The model consists of three terms: a combinatorial, entropic; a residual, enthalpic (short range terms) and the electrostatic (long range) term of Debye–Hückel type, Eq. (13). The model requires volume, r and surface area, q parameters for each species and adjustable binary interaction energy parameters, u_{ki} for each pair of species

$$\frac{g^E}{RT} = \left[\frac{g^E}{RT}\right]_{\text{Combinatorial}} + \left[\frac{g^E}{RT}\right]_{\text{Residual}} + \left[\frac{g^E}{RT}\right]_{\text{Debye-Hückel}} \quad (13)$$

The temperature, T (K), dependence of the interaction energy parameter (ψ_{ki}) of the residual term is given as

$$\psi_{ki} = \exp\left(-\frac{u_{ki} - u_{ii}}{T}\right) \quad (14)$$

where

$$u_{ki} = u_{ki}^0 + u_{ki}^T(T - 298.15) \quad (15)$$

3.4. Thermodynamic parameters

Thermodynamic parameters needed for each of the models are parameters in the activity coefficient model, equilibrium constants and Henry's law constant for CO₂ in pure water. The equilibrium constants are defined in terms of mole fractions, thus they are dimensionless, while the Henry constant has the unit of pascal. The temperature, T (K), dependencies of the equilibrium and Henry's constant used in this work are given by

$$\ln K \text{ or } \ln H = C_1 + C_2/T + C_3 \ln T + C_4 T \quad (16)$$

The coefficients C_1 – C_4 are summarized in Table 2 for all reactions together with literature sources.

3.5. Model parameter regression

CO₂ can be bound chemically by an absorbent or remain as free CO₂ (physical solubility) in an absorbent. Physical solubility of CO₂ into an absorbent at various concentrations and temperatures is necessary in the development of kinetics and thermodynamic models for the system. The problem is that CO₂ reacts with the absorbent. This reactive nature of CO₂ with any absorbent does not allow direct measurement of the physical CO₂ solubility in the solution. The physical solubility is thus measured indirectly using a similar non-reacting gas, N₂O by an analogy, the N₂O analogy. The N₂O analogy was originally proposed by Clarke (1964) and verified by Laddha et al. (1981). It gives a measure of the physical solubility of CO₂ in the aqueous amine solution. It has been applied on various amine systems; Haimour and Sandall (1984), Versteeg and Van Swaaij (1988), Mandal et al. (2005), and Hartono et al. (2008). Previous works that have modeled CO₂ equilibrium in aqueous MEA solutions have not incorporate experimentally determined physical (N₂O) solubility of CO₂ in MEA. The use of N₂O solubility in the model calculations enables determination of the CO₂ activity coefficient. Hessen (2010) showed results of CO₂ activity coefficients calculated by refined-electrolyte–NRTL and extended UNIQUAC for N₂O solubility and compared to experimental values. Results from both models did not agree with experimental result. This work implements the Henry's law constant of CO₂ in MEA, as described by Eq. (19) as data from Hartono (2009) for solubility of N₂O into 30 mass% MEA solution at various CO₂ loadings were included in the parameter regression data set. Expressions for solubility of CO₂ and N₂O in water have been correlated by Versteeg and Van Swaaij (1988) in form of Henry's law constants; where $H_{\text{CO}_2}^w$ and $H_{\text{N}_2\text{O}}^w$ are the Henry's law constants of CO₂ and N₂O in water, respectively, and T (K) is temperature. The solubilities in the mixed MEA/water solvent are given as apparent Henry's law coefficients

$$H_{\text{CO}_2}^w = 2.82 \times 10^6 \exp(-2044/T) \quad (17)$$

$$H_{\text{N}_2\text{O}}^w = 8.55 \times 10^6 \exp(-2284/T) \quad (18)$$

$$H_{\text{CO}_2}^{\text{app,MEA}} = \frac{H_{\text{CO}_2}^w}{H_{\text{N}_2\text{O}}^w} H_{\text{N}_2\text{O}}^{\text{app,MEA}}$$

$$H_{\text{CO}_2}^{\text{app,MEA}} = \gamma_{\text{CO}_2}^* H_{\text{CO}_2}^w \quad (19)$$

Table 2
Mole fraction based temperature dependent equilibrium constants and Henry's law constant for CO₂.

Reaction	Parameter	C ₁	C ₂	C ₃	C ₄	T (°C)	Source
4	$K_{\text{H}_2\text{O}}$	132.899	−13,445.90	−22.4773	0	0–225	Edwards et al. (1978)
5	K_{CO_2}	231.465	−12,092.10	−36.7816	0	0–225	Edwards et al. (1978)
6	$K_{\text{HCO}_3^-}$	216.049	−12,431.70	−35.4819	0	0–225	Edwards et al. (1978)
7	K_{MEA}	−4.9074	−6166.12	0	−0.00098482	0–50	Bates and Pinching (1951)
8	K_{MEACOO^-}	2.8898	−3635.09	0	0	25–120	Austgen et al. (1989)
	H_{CO_2}	170.7126	−8477.711	−21.95743	0.005781	0–100	Chen et al. (1979)

The deviations of the model results from the experimental data are given as absolute average relative deviations (AARD) according

$$AARD = 100\% \frac{1}{n} \sum_n \frac{|x_{model} - x_{exp}|}{x_{exp}} \quad (21)$$

where x is partial pressure, total pressure or apparent Henry's law constant.

4. Results and discussion

Vapor–liquid equilibrium experiment measurement results for 15, 30, 45 and 60 mass% MEA are given in Tables 3–6, respectively, for 40–120 °C. Details of the estimated extended UNIQUAC model volume, r and surface area, q parameters as well as the temperature dependent interaction energy parameters u_{ki}^O and u_{ki}^T regressed using experimentally determined CO₂ partial pressures, total pressures and loadings as well as N₂O solubility data of Hartono (2009) are given in Tables 7–9.

Table 5
Equilibrium solubility of CO₂ in aqueous 45 mass% MEA.

45% MEA															
40 °C		60 °C				80 °C				100 °C			120 °C		
p_{CO_2} (kPa)	α_{CO_2} (mol/mol)	P_{tot} (kPa)	p_{CO_2} (kPa)	$p_{CO_2, model}$ (kPa)	α_{CO_2} (mol/mol)	P_{tot} (kPa)	p_{CO_2} (kPa)	$p_{CO_2, model}$ (kPa)	α_{CO_2} (mol/mol)	P_{tot} (kPa)	$p_{CO_2, model}$ (kPa)	α_{CO_2} (mol/mol)	P_{tot} (kPa)	$p_{CO_2, model}$ (kPa)	α_{CO_2} (mol/mol)
0.0035	0.141		0.0019		0.045		0.0008		0.017	86.6	4.708	0.270	165.1	3.560	0.145
0.0035	0.148		0.0059		0.087		0.0023		0.027	201.7	96.884	0.445	241.5	106.177	0.374
0.0077	0.195		0.0099		0.120		0.0056		0.038	319.4	208.127	0.479	361.5	250.646	0.426
0.0099	0.217		0.0205		0.169		0.0060		0.025	433.3	238.500	0.485	443.7	335.793	0.443
0.0123	0.234		0.0787		0.232		0.0099		0.061	539.0	341.539	0.501	538.7	490.925	0.465
0.0164	0.276		0.1284		0.269		0.0288		0.086	625.4	389.847	0.507	653.1	592.662	0.476
0.0178	0.271		0.4279		0.352		0.0529		0.109	747.2	434.768	0.512	752.2	667.434	0.483
0.0364	0.300		1.4259		0.392		0.1236		0.135	879.5	574.312	0.525	852.7	750.925	0.490
0.0598	0.354		4.6349		0.454		0.3981		0.236	974.6	611.783	0.528	928.9	887.076	0.500
0.1087	0.390		6.2928		0.460		4.5002		0.389	1031.0	693.481	0.534	1039.6	979.386	0.506
0.1781	0.404		8.2900		0.471		11.249		0.435						
0.2787	0.428	56.3		36.099	0.503	97.0		59.190	0.479						
0.9173	0.464	151.8		106.190	0.534	251.9		157.604	0.512						
2.1609	0.475	322.2		264.384	0.567	342.5		279.468	0.533						
5.4871	0.497	422.9		364.534	0.580	446.1		352.012	0.542						
		509.9		421.021	0.586	523.8		419.045	0.549						
		627.9		612.781	0.602	624.4		509.029	0.557						
		714.6		771.31		714.8		615.796	0.565						
		868.0		947.05		842.1		725.466	0.572						
		1030.4		1243.31		941.5		872.797	0.580						
						1039.8		1121.96	0.591						

Table 6
Equilibrium solubility of CO₂ in aqueous 60 mass% MEA.

60% MEA											
40 °C		60 °C		80 °C		100 °C			120 °C		
p_{CO_2} (kPa)	α_{CO_2} (mol/mol)	p_{CO_2} (kPa)	α_{CO_2} (mol/mol)	p_{CO_2} (kPa)	α_{CO_2} (mol/mol)	P_{tot} (kPa)	$p_{CO_2, model}$ (kPa)	α_{CO_2} (mol/mol)	P_{tot} (kPa)	$p_{CO_2, model}$ (kPa)	α_{CO_2} (mol/mol)
0.0060	0.173	0.0007	0.046	0.0020	0.018	106.3	30.942	0.386	196.9	77.117	0.346
0.0127	0.242	0.0110	0.126	0.0170	0.056	204.9	78.602	0.430	306.0	185.399	0.398
0.0281	0.306	0.0341	0.172	0.0325	0.073	308.6	126.628	0.450	412.3	306.435	0.426
0.0526	0.344	0.1097	0.248	0.0777	0.124	414.6	226.909	0.473	537.0	395.997	0.440
0.1508	0.394	0.2933	0.316	0.1610	0.162	518.3	279.632	0.481	700.0	551.896	0.458
0.3824	0.427	0.8475	0.382	0.2513	0.191	618.4	438.671	0.498	963.3	845.133	0.481
0.9062	0.449	3.0267	0.424	0.5431	0.238	705.0	529.194	0.505	1060.2	945.232	0.487
1.5153	0.468	8.2258	0.457	0.8699	0.264						
3.7472	0.481	18.967	0.480	1.6522	0.308						
12.472	0.500			3.4300	0.352						
				6.0947	0.387						
				9.0463	0.404						
				11.271	0.416						

4.1. Binary H₂O–MEA system

Vapor–liquid equilibrium for the binary H₂O–MEA system was not measured in this work. However, sample model predicted results for the binary H₂O–MEA system are given as Pxy diagrams in Fig. 3a and compared with experimental results of Tochigi et al. (1999) and Belabbaci et al. (2009) while activity coefficients are given in Fig. 3b and compared with experimental results of Belabbaci et al. (2009) and Kim et al. (2008). Fig. 4a shows results for model prediction of excess enthalpy of MEA compared to data from Touhara et al. (1982) and Posey (1996). Freezing point depression predictions compared to data from Chang et al. (1993) are shown in Fig. 4b. These results confirm that the e-UNIQUAC implementation of this work is consistent with the work of Faramarzi et al. (2009) from which the interaction parameters for the binary H₂O–MEA system were gathered. Quantitative agreement between literature and model prediction of different properties of H₂O–MEA system expressed as percent AARD values are given in Table 10.

Table 7
UNIQUAC volume, r and surface area, q parameters.

Species	r	q	Source
H ₂ O	0.9200	1.4000	Abrams and Prausnitz (1975)
MEA	4.2800	4.2800	Faramarzi et al. (2009)
CO ₂	5.7410	6.0806	Thomsen and Rasmussen (1999)
H ₃ O ⁺	0.13779	1.0E–15	Thomsen et al. (1996)
MEAH ⁺	1.0241	2.5150	This work
OH [–]	9.3973	8.8171	Thomsen et al. (1996)
HCO ₃ [–]	9.1571	6.3461	This work
CO ₃ ^{2–}	9.7452	6.4614	This work
MEACOO [–]	1.0741	0.1106	This work

4.2. Ternary H₂O–MEA–CO₂ system

The extended UNIQUAC model results for the N₂O (physical) solubility of 30 mass% MEA are shown in Fig. 5. Fig. 5a shows that the model adequately correlates the experimental Henry's law constant of CO₂ in MEA. The activity coefficient of CO₂ is thus well represented by the model up to the loading of 0.5 measured by Hartono (2009). In Fig. 5b a parity plot is given. The AARD value of 2.7% indicates a very good representation of experimental data.

Model calculations and experimental CO₂ partial pressures from this work as functions of loading and temperature are given

Table 8
UNIQUAC interaction energy parameters for $u_{ij} = u_{ij}^0 + u_{ij}^T(T - 298.15)$; $u_{ij}^0 = u_{ji}^0$.

	H ₂ O	MEA	CO ₂	H ₃ O ⁺	MEAH ⁺	OH [–]	HCO ₃ [–]	CO ₃ ^{2–}	MEACOO [–]
H ₂ O	0.0000								
MEA	173.9645	414.6924							
CO ₂	–151.4573	87.5583	40.5176						
H ₃ O ⁺	1.0E+04	1.0E+09	1.0E+09	0.0000					
MEAH ⁺	–20.7732	310.1293	30.8035	1.0E+09	0.0000				
OH [–]	600.4952	1.0E+09	2500.0000	1.0E+09	1.0E+09	1562.8810			
HCO ₃ [–]	517.0278	655.0881	597.9726	1.0E+09	732.7007	2500.0000	743.6159		
CO ₃ ^{2–}	361.3877	1.0E+09	2500.0000	1.0E+09	1.0E+09	1588.0250	719.159	1458.3440	
MEACOO [–]	2758.3852	1.0E+09	1.0E+09	1.0E+09	1.0E+09	1.0E+09	1.0E+09	1.0E+09	1500.0000

Bold: Thomsen and Rasmussen (1999); Italics: Faramarzi et al. (2009); Non-italics: Regressed, this work.

Table 9
UNIQUAC interaction energy parameters for $u_{ij} = u_{ij}^0 + u_{ij}^T(T - 298.15)$; $u_{ij}^T = u_{ji}^T$.

	H ₂ O	MEA	CO ₂	H ₃ O ⁺	MEAH ⁺	OH [–]	HCO ₃ [–]	CO ₃ ^{2–}	MEACOO [–]
H ₂ O	0.0000								
MEA	0.8027	0.6647							
CO ₂	6.0908	4.6660	13.6290						
H ₃ O ⁺	0.0000	0.0000	0.0000	0.0000					
MEAH ⁺	–1.9174	0.1213	7.3541	0.0000	0.0000				
OH [–]	8.5455	0.0000	0.0000	0.0000	0.0000	5.6169			
HCO ₃ [–]	6.9504	15.2488	5.8077	0.0000	2.8863	0.0000	17.1148		
CO ₃ ^{2–}	3.3516	0.0000	0.0000	0.0000	0.0000	2.7496	2.6115	–1.3448	
MEACOO [–]	16.9192	0.0000	0.0000	0.0000	0.0000	0.0000	0.0000	0.0000	0.0000

Bold: Thomsen and Rasmussen (1999); Italics: Faramarzi et al. (2009); Non-italics: Regressed, this work.

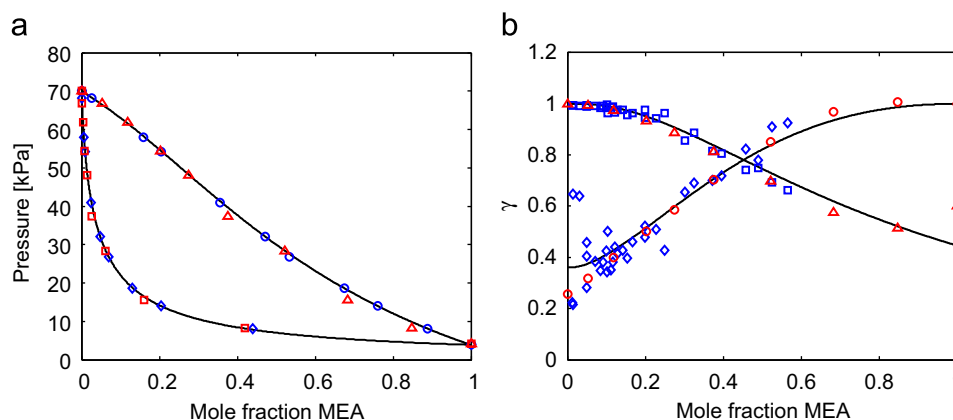


Fig. 3. (a) Pxy diagram for H₂O–MEA system; 90 °C: vapor phase mole fraction (○, Tochigi et al., 1999; △, Belabbaci et al., 2009); liquid phase mole fraction (◇, Tochigi et al., 1999; □, Belabbaci et al., 2009). Lines, model predictions. (b) H₂O–MEA activity coefficient, 60 °C: H₂O (□, Kim et al., 2008; △, Belabbaci et al., 2009); MEA (◇, Kim et al., 2008; ○, Belabbaci et al., 2009). –, model predictions.

in Fig. 6 while Fig. 7 shows model calculations and experimental total pressures. The results show the robustness of the model. It correlates well CO₂ partial pressures and total pressures over MEA solutions for 15, 30, 45 and 60 mass% MEA. The parity plot between experimental data and model predicted pressure are given in Fig. 8. Fig. 8a shows parity plot results from this work as well as for data for low MEA concentrations; 0.6, 3.0 and 6.0 mass% MEA. The figure shows that the model predicts the CO₂ partial pressure very well even at very low MEA concentrations. The data for the low MEA concentrations were not used in the parameter regression, but serve for validation of the implemented model. Fig. 8a thus shows that the model accurately calculates CO₂ equilibrium in MEA at all concentration ranges up to 60 mass%. Fig. 8b shows a parity plot where a range of data for 30 mass% from the literature is included. The figure indicates that the model is able to correlate existing equilibrium data for H₂O–MEA–CO₂ system in a good manner. However, the CO₂ partial pressure data of Goldman and Leibush (1959) and Shen and Li (1992) are in general somewhat high, and thus are under-predicted by the model, while the data of Lee et al. (1976) and Jou et al. (1995) are somewhat low, and thus are generally over-predicted by the model. Other literature data represented are Hilliard (2008) and Xu and Rochelle (2011). The experimental data from this work is observed to lie between the above mentioned data sets. Hessen (2010) discussed whether the data of Jou et al. (1995) at absorber conditions indicated too low partial pressures. The background for this discussion was that an implementation of an equilibrium model based on these data into the rate-based CO₂SIM simulator gave too low partial pressures compared with pilot plant data. It is therefore interesting that the

Table 10

Quantitative agreement between literature and model prediction of different properties of H₂O–MEA system expressed as percent AARD.

Literature	Total pressure	Activity coefficient	Excess enthalpy	Freezing point depression
Kim et al. (2008)	1.06	10.48		
Tochigi et al. (1999)	0.86	7.99		
Touhara et al. (1982)			8.97	
Posey (1996)			4.25	
Chang et al. (1993)				2.41

data obtained in this work can be seen to represent a trade-off between different sets of data from the literature. The overall average absolute relative deviation (AARD) of 16.2% for the fit to own data shows that the model gives a good representation of the experimental data used in the regression analysis. The AARD value for fit to CO₂ partial pressures and total pressures for all MEA concentrations were 24.3% and 11.7%, respectively. The parity plot of the ratio between the model results to the experimental pressure results, $P_{model}/P_{experiment}$, for the data used in the model regression is shown in Fig. 9. The figure shows that the data points are well distributed by the model.

Fig. 10 shows the concentration dependency of CO₂ partial pressure for the H₂O–MEA–CO₂ system as determined by experiment and model calculations. It is clear from Fig. 10a that CO₂ partial pressures over MEA solution do show a dependency on MEA concentration at loadings less than 0.5 mol CO₂/mol MEA where CO₂ partial pressure is observed to decrease with increase in MEA concentration. The equilibrium curves are observed to “straighten up” with increase in concentration showing a strong concentration dependency at higher loadings where equilibrium CO₂ partial pressures are found to increase with increase in amine concentration and CO₂ loading in Fig. 10b. Cross over of the curves is observed to occur at about 0.45 loading as shown in Fig. 10a. A strong dependency of CO₂ partial pressure on amine concentration at high loadings has been predicted and observed by Austgen et al. (1989) and Dugas (2009), respectively. A further analysis of the experiment and model correlation in the low loading region was carried out using a plot of the residuals as function of MEA concentration within a narrow loading range (0.05–0.15 mol CO₂/mol MEA) as shown in Fig. 11. The figure shows a random distribution of the residual points. This indicates a good correlation of the experimental data by the model also for this region.

4.3. Speciation

Liquid phase concentration of the different species is necessary in kinetic expressions for mass-transfer at the liquid–vapor interfaces. The model speciation results at 40 °C are compared with literature NMR results from Poplsteinova et al. (2005), Böttlinger et al. (2008) and Hilliard (2008) in Fig. 12. The model results show good agreement with experimental data for the main components MEA, MEAH⁺, CO₂, HCO₃⁻ and MEACOO⁻.

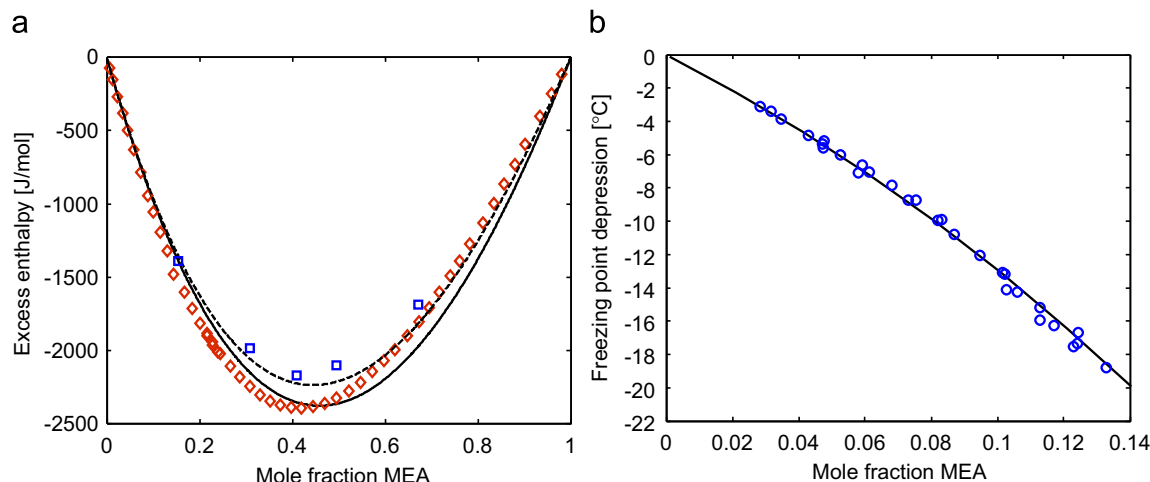


Fig. 4. (a) Excess enthalpy H₂O–MEA; 25 °C: \diamond , Touhara et al. (1982); line, model prediction; 69.4 °C: \square , Posey (1996); dashed line, model prediction. (b) Freezing point depression, H₂O–MEA: \circ , Chang et al. (1993); —, model predictions.

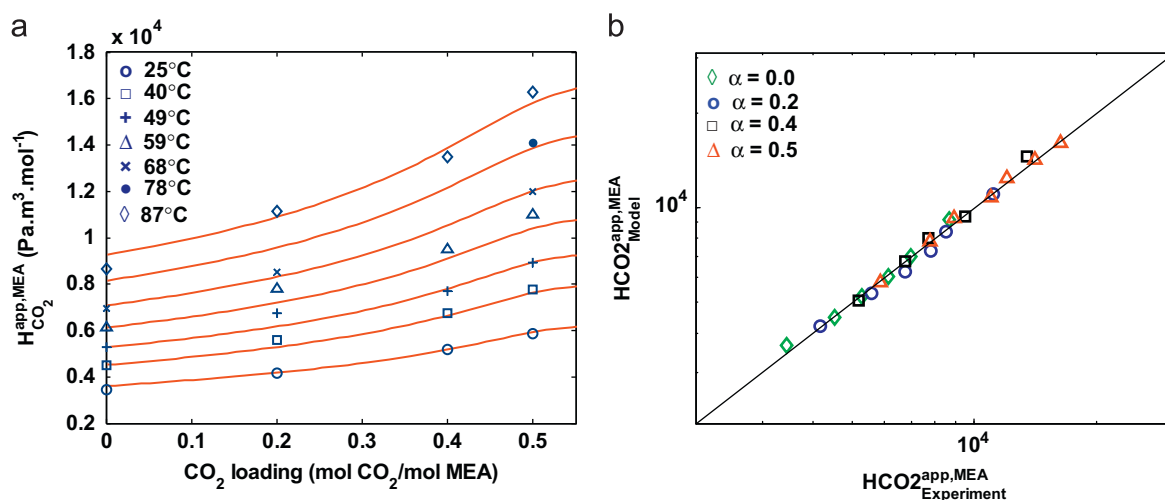


Fig. 5. (a) Apparent Henry's law constant of CO₂ in 30 mass% MEA at various CO₂ loadings. Experimental points, Hartono (2009); Lines, model prediction. (b) Parity plot between experimental and model predictions of apparent Henry's law constant of CO₂ in 30 mass% MEA.

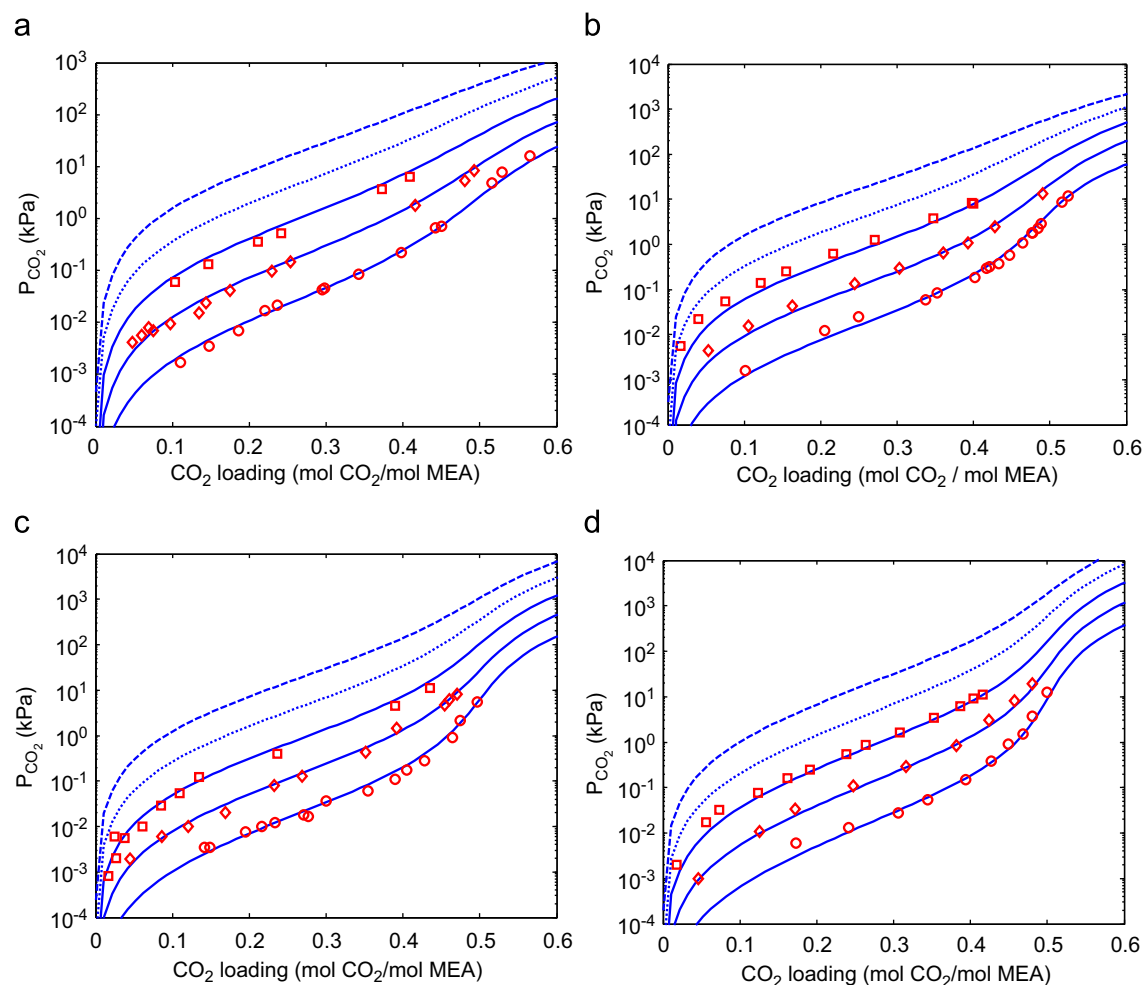


Fig. 6. CO₂ partial pressure as function of loading for H₂O-MEA-CO₂ system. Experimental data: ○, 40 °C; ◇, 60 °C; □, 80 °C; ---, 100 °C, model prediction; — — —, 120 °C, model prediction: (a) 15 mass% MEA, (b) 30 mass% MEA, (c) 45 mass% MEA, and (d) 60 mass% MEA.

The model predictions for CO₃²⁻ are lower than the Poplsteinova et al. (2005) results. This may well be due to difficulties in distinguishing between HCO₃⁻ and CO₃²⁻ in the experiments.

Poplsteinova et al. (2005) relied on changes in chemical shift with pH and temperature to predict the individual HCO₃⁻ and CO₃²⁻ concentrations. It indicated that the concentration of carbonate

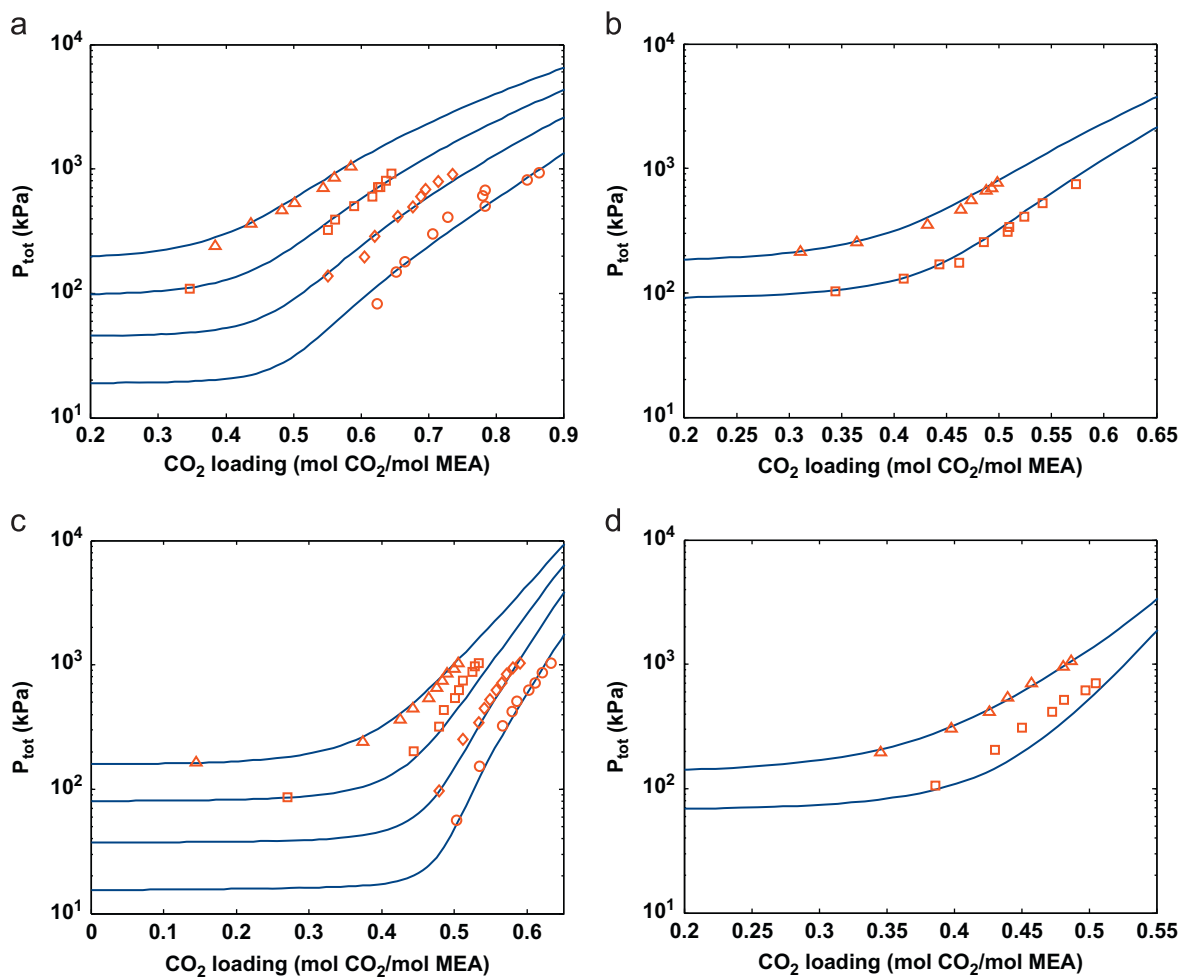


Fig. 7. Total pressure as function of loading for H_2O –MEA– CO_2 system. Experimental data: \circ , 60 °C; \diamond , 80 °C; \square , 100 °C; \triangle , 120 °C; Lines, model: (a) 15 mass% MEA, (b) 30 mass% MEA, (c) 45 mass% MEA, and (d) 60 mass% MEA.

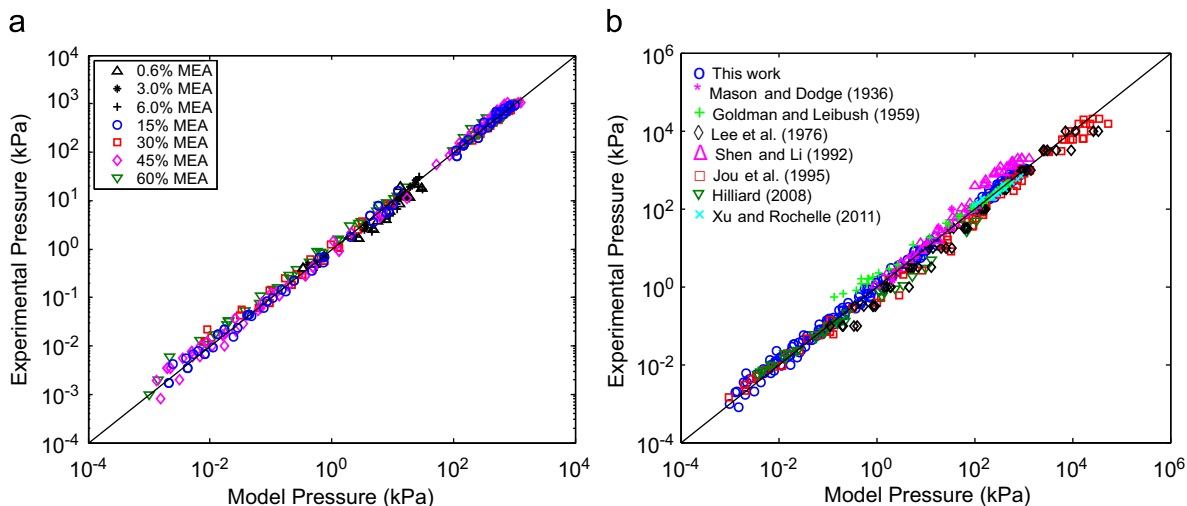


Fig. 8. (a) Parity plot between experimental and model predicted pressures and (b) parity plot between experimental data from this work and from literature and model predicted pressures.

was most likely significantly over-predicted. The lower concentrations of CO_3^{2-} as predicted in this work thus may give a better representation of the real carbonate concentration. This is,

however, uncertain. Böttlinger et al. (2008) reported values for HCO_3^- and CO_3^{2-} , but it is not clear if these values are the sum of $\text{HCO}_3^-/\text{CO}_3^{2-}$. It also reported a combined MEA/MEA $^+$ result.

The speciation results as given in this work seem to be an improvement on results from Faramarzi et al. (2009), where HCO_3^- concentrations most likely were over-predicted, as was further discussed by Hessen (2010).

The heat of absorption of CO_2 in an absorbent, ΔH_{abs} , can be accurately determined by calorimetric measurements using a method differential in temperature and semi-differential in loading, Kim and Svendsen (2007). The model in this work can calculate rigorously the heat of absorption of CO_2 into aqueous MEA system. However, as an estimate, the Gibbs–Helmholtz equation, Eq.(22) is used. As pointed out by Kim and Svendsen (2007), this method does not necessarily give an accurate description of the ΔH_{abs} values

$$\left(\frac{\partial \ln p_{\text{CO}_2}}{\partial (1/T)}\right)_{p,x} = \frac{-\Delta H_{\text{abs}}}{R} \quad (22)$$

Fig. 13 shows the result for the estimated, temperature independent heat of absorption calculated from the VLE model. The figure shows that the estimated heat of absorption for MEA

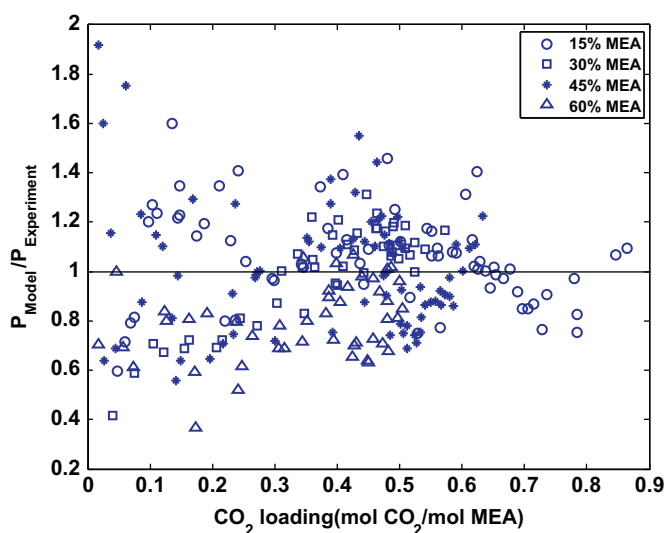


Fig. 9. Parity plot for the ratio between the model results and the experimental pressures used in model regression as a function of CO_2 loading.

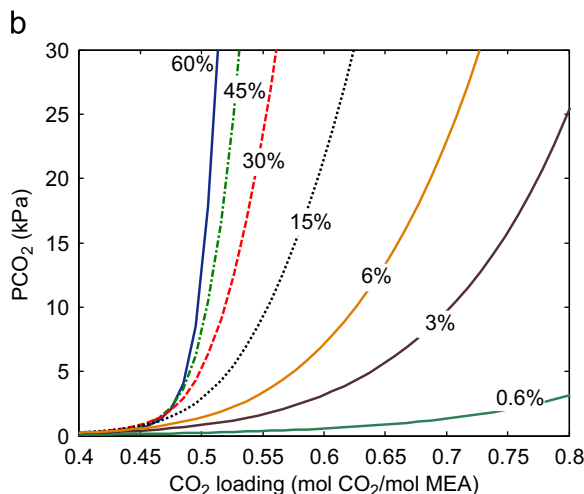
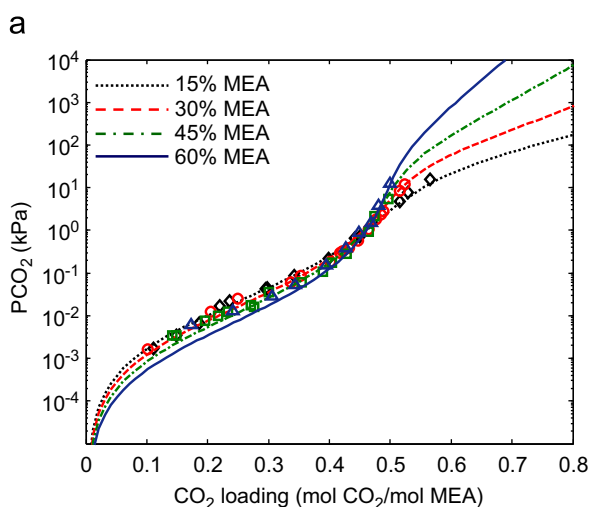


Fig. 10. Concentration dependency of equilibrium CO_2 partial pressure of H_2O –MEA– CO_2 system at 40°C .

agrees fairly well with experimental results of Kim (2009), considering that the model does not calculate the values rigorously (Kim et al., 2009).

Fig. 14 shows the model predictions of MEA volatility where the partial pressures of MEA and H_2O for 30 mass% MEA are compared with experimental data of Hilliard (2008). The model is seen to predict well both partial pressures at 60°C and also the partial pressure of water at 40°C , but it under-predicts the values for MEA at 40°C . Similar results were obtained for MEA using the e-NRTL model by Hessen (2010). One may still raise a question regarding the accuracy of the data for MEA at 40°C , in particular at high loadings where the partial pressures of MEA are very low.

5. Conclusions

New experimental data for vapor–liquid equilibrium of CO_2 in aqueous monoethanolamine solutions are presented for 15, 30, 45 and 60 mass% MEA and from 40 to 120°C . CO_2 partial pressures over loaded MEA solutions were measured using a low temperature equilibrium apparatus while total pressures were measured with a

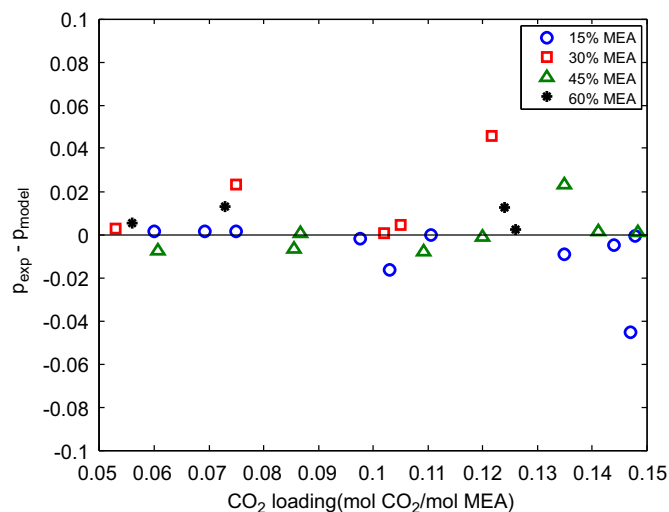


Fig. 11. Residuals a function of MEA concentration over very narrow loading range 0.05 – 0.15 mol CO_2 /mol MEA.

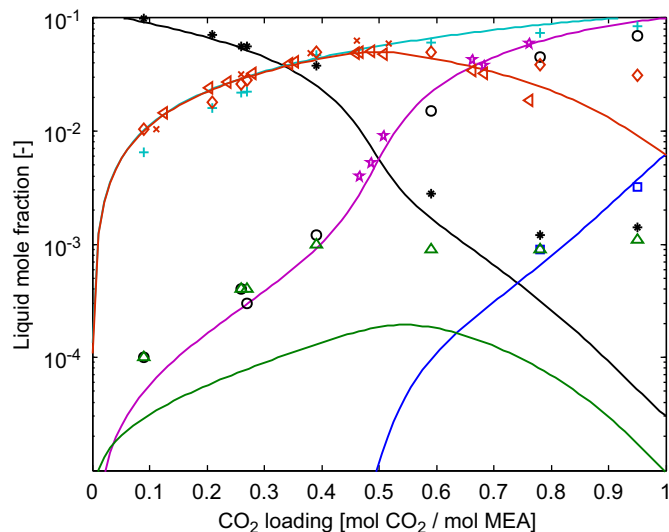


Fig. 12. Liquid phase speciation in 30 mass% MEA at 40 °C. *, MEA; □, CO₂; +, MEAH⁺; ○, HCO₃⁻; △, CO₃²⁻; ◇, MEACOO⁻; Poplsteinova et al. (2005) ★, HCO₃⁻; ▽, MEACOO⁻; Böttinger et al. (2008). ×, MEACOO⁻; Hilliard (2008). Lines; model prediction.

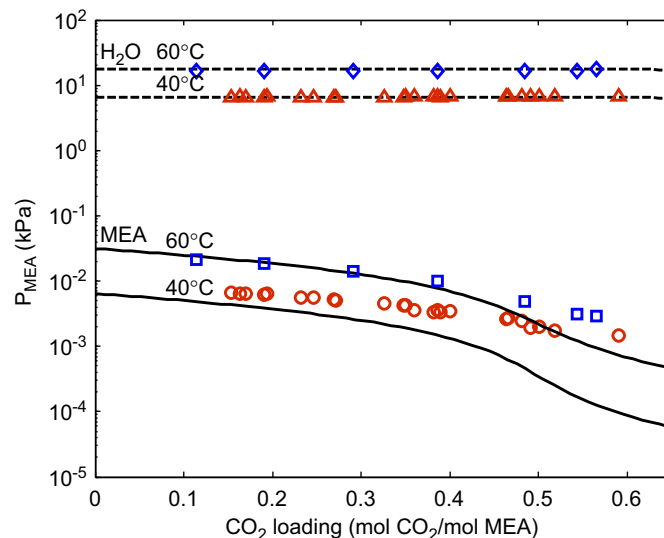


Fig. 14. Model prediction of partial pressures (volatility) of MEA and H₂O in a H₂O–MEA–CO₂ system. Lines: model prediction; Experimental data: Hilliard (2008).

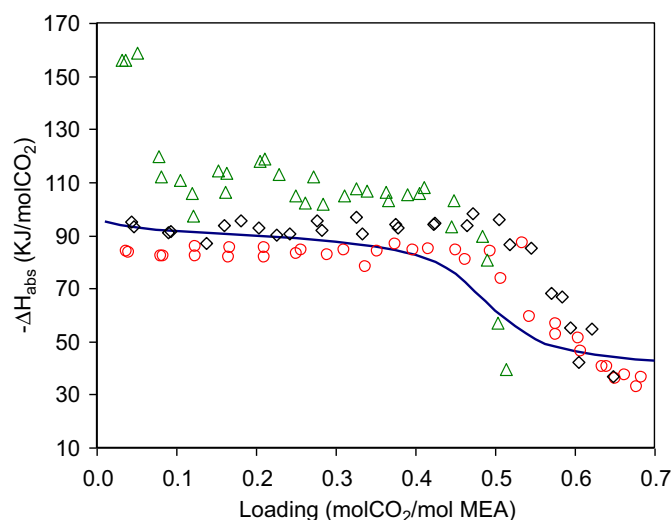


Fig. 13. Estimated heat of absorption of CO₂ into 30 mass% MEA; experimental points: ○, 40 °C; ◇, 80 °C; △, 120 °C, Kim (2009). Line; model prediction.

high temperature equilibrium apparatus. The extended UNIQUAC model framework was applied; model parameters were fitted to the new experimental VLE data and physical solubility data from the literature. The model gives a good representation of the experimental VLE data for CO₂ partial pressure and total pressures for all MEA concentrations with average absolute relative deviation (AARD) of 24.3% and 11.7%, respectively, while the physical solubility data was represented with an AARD of 2.7%. Further, the model predicts well liquid phase speciation results determined by NMR and experimental data for freezing point depression and excess enthalpy.

Nomenclature

AARD	average absolute relative deviation
F	objective function
g	specific Gibbs energy (J mol ⁻¹)
H	Henry's law constant (Pa m ³ mol ⁻¹)

K	equilibrium constant
NMR	nuclear magnetic resonance
n	mole number; number of elements
P	total pressure (kPa)
p	partial pressure (kPa)
q	UNIQUAC surface area parameter
R	universal gas constant (J mol ⁻¹ K ⁻¹)
r	UNIQUAC volume parameter
T	temperature (K)
u	UNIQUAC interaction parameter
v	molar volume (m ³ mol ⁻¹)
ν	stoichiometric coefficient
x	liquid phase mole fraction, partial pressure, total pressure, Henry's law constant
y	vapor phase mole fraction

Greek letters

ΔH_{abs}	heat of absorption of CO ₂ (kJ/mol CO ₂)
θ	UNIQUAC surface fraction
μ	chemical potential
ϕ	fugacity coefficient
ϕ	UNIQUAC volume fraction
ψ	auxiliary function (UNIQUAC)
u	UNIQUAC interaction energy parameter

Subscripts

i	component i
j	species counter
k	species counter
model	model calculated
tot	total
ν	stoichiometric coefficient
w	water
∞	infinite dilution

Superscripts

app	apparent
calc	model calculated

exp	experimental
E	excess
IR	infra red analyzer
liq	liquid phase
o	standard state; temperature independent
s	saturated
T	temperature dependent
vap	vapor phase
w	water
*	asymmetrical
∞	infinite dilution

Acknowledgments

This publication forms a part of the BIGCO₂ project, performed under the strategic Norwegian research program Climit. The authors acknowledge the partners: Statoil AS, GE Global Research, Statkraft, Aker Clean Carbon, Shell, TOTAL, ConocoPhillips, ALSTOM, the Research Council of Norway (178004/I30 and 176059/I30) and Gassnova.

References

- Abrams, D.S., Prausnitz, J.M., 1975. Statistical thermodynamics of liquid mixtures. New expression for the excess Gibbs energy of partly or completely miscible systems. *AIChE J.* 21 (1), 116–128.
- Aronu, U.E., Hoff, K.A., Svendsen, H.F., 2011a. Vapor–liquid equilibrium in aqueous amine amino acid salt solution: 3-(methylamino)propylamine/sarcosine. *Chem. Eng. Sci.* 66 (17), 3859–3867.
- Aronu, U.E., Hessen, E.T., Haug-Warberg, T., Hoff, K.A., Svendsen, H.F., 2011b. Vapor–liquid equilibrium in amino acid salt system: experiments and modeling. *Chem. Eng. Sci.* 66 (10), 2191–2198.
- Atadan, E.M., 1954. Absorption of Carbon Dioxide by Aqueous Monoethanolamine Solutions. Ph.D. Thesis. University of Tennessee, Knoxville, TN.
- Austgen, D.M., Rochelle, G.T., Peng, X., Chen, C.C., 1989. Model of vapor–liquid equilibria for aqueous acid gas–alkanolamine systems using the electrolyte–NRTL equation. *Ind. Eng. Chem. Res.* 28 (7), 1060–1073.
- Bates, R.G., Pinching, G.D., 1951. Acidic dissociation constant and related thermodynamic quantities for monoethanolammonium ion in water from 0° to 50 °C. *J. Res. Natl. Bur. Stand.* 46, 349–352.
- Belabbaci, A., Razzouk, A., Mokbel, I., Jose, J., Negadi, L., 2009. Isothermal vapor–liquid equilibria of (monoethanolamine + water) and (4-methylmorpholine + water) binary systems at several temperatures. *J. Chem. Eng. Data* 54 (8), 2312–2316.
- Brelvi, S.W., O’Connell, J.P., 1972. Corresponding states correlations for liquid compressibility and partial molal volumes of gases at infinite dilution in liquids. *AIChE J.* 18 (6), 1239–1243.
- Bouillon, P.A., Lemaire, E., Mangiaracina A., Tabasso C., 2011. First results of the 2.25 t/h post-combustion CO₂ capture pilot plant of ENEL at the Brindisi Coal Power Plant with MEA from 20 to 40 %wt. In: Proceedings of the First Post-Combustion Capture Conference (PCCC1), 17–19 May, Abu Dhabi.
- Böttinger, W., Maiwald, M., Hasse, H., 2008. Online NMR spectroscopic study of species distribution in MEA–H₂O–CO₂ and DEA–H₂O–CO₂. *Fluid Phase Equilibria* 263 (2), 131–143.
- Chang, H.T., Posey, M., Rochelle, G.T., 1993. Thermodynamics of alkanolamine–water solutions from freezing point measurements. *Ind. Eng. Chem. Res.* 32 (10), 2324–2335.
- Chen, C.-C., Britt, H.I., Boston, J.F., Evans, L.B., 1982. Local composition model for excess Gibbs energy of electrolyte systems, Part I: single solvent, single completely dissociated electrolyte systems. *AIChE J.* 28 (4), 588–596.
- Chen, C.C., Evans, L.B., 1986. A local composition model for the excess Gibbs energy of aqueous electrolyte systems. *AIChE J.* 32 (3), 444–454.
- Chen, C.-C., Britt, H.I., Boston, J.F., Evans, L.B., 1979. Extension and application of the Pitzer equation for vapor–liquid equilibrium of aqueous electrolyte systems with molecular solutes. *AIChE J.* 25 (5), 820–831.
- Clarke, J.K.A., 1964. Kinetics of absorption of carbon dioxide in monoethanolamine solutions at short contact times. *Ind. Eng. Chem. Fund.* 3 (3), 239–245.
- Deshmukh, R.D., Mather, A.E., 1981. A mathematical model for equilibrium solubility of hydrogen sulfide and carbon dioxide in aqueous alkanolamine solutions. *Chem. Eng. Sci.* 36 (2), 355–362.
- Dugas, R.E., 2009. Carbon Dioxide Absorption, Desorption, and Diffusion in Aqueous Piperazine and Monoethanolamine. Ph.D. Dissertation. The University of Texas at Austin.
- Edwards, T.J., Maurer, G., Newman, J., Prausnitz, J.M., 1978. Vapor–liquid equilibria in multicomponent aqueous solutions of volatile weak electrolytes. *AIChE J.* 24 (6), 966–976.
- Faramarzi, L., Kontogeorgis, G.M., Thomsen, K., Stenby, E.H., 2009. Extended UNIQUAC model for thermodynamic modeling of CO₂ absorption in aqueous alkanolamine solutions. *Fluid Phase Equilibria* 282 (2), 121–132.
- Goldman, A.M., Leibush, A.G., 1959. A study of the equilibrium of carbon dioxide desorption of monoethanolamine solution in the temperature range 75–140 °C. *Tr. Gos. Nauchno-Issled. Proektn. Inst. Azotn. Promsti* 10, 53–82.
- Haimour, N., Sandall, O.C., 1984. Absorption of carbon dioxide into aqueous methyl-diethanolamine. *Chem. Eng. Sci.* 39 (12), 1791–1796.
- Hartono, A., 2009. Characterization of Diethylenetriamine (DETA) as Absorbent for Carbon Dioxide. Ph.D. Thesis. Norwegian University of Science and Technology.
- Hartono, A., Juliusen, O., Svendsen, H.F., 2008. Solubility of N₂O in aqueous solution of diethylenetriamine. *J. Chem. Eng. Data* 53 (11), 2696–2700.
- Hertzberg, T., Mejdell, T., 1998. MODFIT for MATLAB Parameter Estimation in a Nonlinear Multiresponse Model. Norwegian University of Science and Technology.
- Hessen, E.T., 2010. Thermodynamic Models for CO₂ Absorption. Ph.D. Thesis. Norwegian University of Science and Technology.
- Hessen, E.T., Haug-Warberg, T., Svendsen, H.F., 2010. The refined e-NRTL model applied to CO₂–H₂O–alkanolamine systems. *Chem. Eng. Sci.* 65 (11), 3638–3648.
- Hilliard, M., 2008. A Predictive Thermodynamic Model for an Aqueous Blend of Potassium Carbonate, Piperazine, and Monoethanolamine for Carbon dioxide. Ph.D. Thesis. The University of Texas at Austin.
- Jou, F.-Y., Mather, A.E., Otto, F.D., 1995. The solubility of CO₂ in a 30 mass percent monoethanolamine solution. *Can. J. Chem. Eng.* 73 (1), 140–147.
- Kent, R.L., Eisenberg, B., 1976. Better data for amine treating. *Hydrocarbon Processing* (1966–2001) 55 (2), 87–90.
- Kim, I., 2009. Heat of Reaction and VLE of Post Combustion CO₂ Absorbents. Ph.D. Thesis. Chemical Engineering Department, Norwegian University of Science and Technology, Trondheim, Norway.
- Kim, I., Hoff, K.A., Hessen, E.T., Haug-Warberg, T., Svendsen, H.F., 2009. Enthalpy of absorption of CO₂ with alkanolamine solutions predicted from reaction equilibrium constants. *Chem. Eng. Sci.* 64 (9), 2027–2038.
- Kim, I., Svendsen, H.F., 2007. Heat of absorption of carbon dioxide (CO₂) in monoethanolamine (MEA) and 2-(aminoethyl) ethanolamine (AEEA) solutions. *Ind. Eng. Chem. Res.* 46 (17), 5803–5809.
- Kim, I., Svendsen, H.F., Borresen, E., 2008. Ellubliometric determination of vapor–liquid equilibria for pure water, monoethanolamine, n-methyldiethanolamine, 3-(methylamino)-propylamine, and their binary and ternary solutions. *J. Chem. Eng. Data* 53 (11), 2521–2531.
- Kohl, A.L., Nielsen, R., 1997. Gas Purification fifth ed Gulf Publishing Company, Houston, Texas.
- Laddha, S.S., Diaz, J.M., Danckwerts, P.V., 1981. The nitrous oxide analogy: the solubilities of carbon dioxide and nitrous oxide in aqueous solutions of organic compounds. *Chemical Engineering Science* 36 (1), 228–229.
- Lee, J.I., Otto, F.D., Mather, A.E., 1976. Equilibrium between carbon dioxide and aqueous monoethanolamine solutions. *Journal of Applied Chemistry & Biotechnology* 26 (10), 541–549.
- Ma’mun, S., Jakobsen, J.P., Svendsen, H.F., Juliusen, O., 2006. Experimental and modeling study of the solubility of carbon dioxide in aqueous 30 mass% 2-((2-aminoethyl)amino)ethanol solution. *Ind. Eng. Chem. Res.* 45 (8), 2505–2512.
- Ma’mun, S., Nilsen, R., Svendsen, H.F., Juliusen, O., 2005. Solubility of carbon dioxide in 30 mass% monoethanolamine and 50 mass% methyldiethanolamine solutions. *J. Chem. Eng. Data* 50 (2), 630–634.
- Mandal, B.P., Kundu, M., Bandyopadhyay, S.S., 2005. Physical solubility and diffusivity of N₂O and CO₂ into aqueous solutions of (2-amino-2-methyl-1-propanol + monoethanolamine) and (N-methyldiethanolamine + monoethanolamine). *J. Chem. Eng. Data* 50 (2), 352–358.
- Mason, J.W., Dodge, B.F., 1936. Equilibrium absorption of carbon dioxide by solutions of the ethanolamines. *Trans. Am. Inst. Chem. Eng.* 32, 27–48.
- Nicolaisen, H., Rasmussen, P., Soerensen, J.M., 1993. Correlation and prediction of mineral solubilities in the reciprocal salt system (Na⁺, K⁺)(Cl⁻, SO₄²⁻)–water at 0–100 °C. *Chem. Eng. Sci.* 48 (18), 3149–3158.
- Poplsteinova, J.J., Krane, J., Svendsen, H.F., 2005. Liquid-phase composition determination in CO₂–H₂O–alkanolamine systems: an NMR study. *Ind. Eng. Chem. Res.* 44 (26), 9894–9903.
- Posey, M.L., 1996. Thermodynamic Model for Acid Gas Loaded Aqueous Alkanolamine Solutions. Ph.D. Thesis. The University of Texas at Austin.
- Sander, B., Fredenslund, A., Rasmussen, P., 1986. Calculation of vapor–liquid equilibria in mixed solvent/salt systems using an extended UNIQUAC equation. *Chem. Eng. Sci.* 41 (5), 1171–1183.
- Shen, K.P., Li, M.H., 1992. Solubility of carbon dioxide in aqueous mixtures of monoethanolamine with methyldiethanolamine. *J. Chem. Eng. Data* 37 (1), 96–100.
- Smith, W.R., Missen, R.W., 1982. Chemical Reaction Equilibrium Analysis: Theory and Algorithms, second ed. Wiley, New York.
- Solbraa, E., 2002. Equilibrium and Non-Equilibrium. Thermodynamics of Natural Gas Processing: Measurement and Modelling of Absorption of Carbon Dioxide into Methyldiethanolamine Solutions at High Pressures. Ph.D. Thesis. Norwegian University of Science and Technology.
- Thomsen, K., 1997. Aqueous Electrolytes: Model Parameters and Process Simulation. Ph.D. Thesis. Technical University of Denmark.

- Thomsen, K., Rasmussen, P., 1999. Modeling of vapor–liquid–solid equilibrium in gas–aqueous electrolyte systems. *Chem. Eng. Sci.* 54 (12), 1787–1802.
- Thomsen, K., Rasmussen, P., Gani, R., 1996. Correlation and prediction of thermal properties and phase behavior for a class of aqueous electrolyte systems. *Chem. Eng. Sci.* 51 (14), 3675–3683.
- Tochigi, K., Akimoto, K., Ochi, K., Liu, F., Kawase, Y., 1999. Isothermal vapor–liquid equilibria for water+2-aminoethanol+dimethyl sulfoxide and its constituent three binary systems. *J. Chem. Eng. Data* 44 (3), 588–590.
- Touhara, H., Okazaki, S., Okino, F., Tanaka, H., Ikari, K., Nakanishi, K., 1982. Thermodynamic properties of aqueous mixtures of hydrophilic compounds. 2. Aminoethanol and its methyl derivatives. *J. Chem. Thermodyn.* 14 (2), 145–156.
- Versteeg, G.F., Van Swaaij, W.P.M., 1988. Solubility and diffusivity of acid gases (carbon dioxide, nitrous oxide) in aqueous alkanolamine solutions. *J. Chem. Eng. Data* 33 (1), 29–34.
- Xu, Q., Rochelle, G., 2011. Total pressure and CO₂ solubility at high temperature in aqueous amines. *Energy Procedia* 4, 117–124.